IEEE Trans. Microwave Theory Tech., vol. MTT-24, pp. 879–881, Nov. 1976.

[6] T. Itanami and S. Shindo, "Channel dropping filter for millimeter-wave integrated circuits," *IEEE Trans. Microwave Theory Tech.*, vol. MTT-26, pp. 759–764, Oct. 1978.

[7] J. A. Paul and Y. Chang, "Millimeter-wave image-guide integrated passive devices," *IEEE Trans. Microwave Theory Tech.*, vol. MTT-26, pp. 751–754, Oct. 1978.

[8] J. A. Paul and P. C. Yen, "Millimeter-wave passive components and six-port network analyzer in dielectric waveguide," *IEEE Trans. Microwave Theory Tech.*, vol. MTT-29, pp. 948–953, Sept. 1981.

[9] R. Rudokas and T. Itoh, "Passive millimeter-wave IC components made of inverted strip dielectric waveguides," *IEEE Trans. Microwave Theory Tech.*, vol. MTT-24, pp. 978–981, Dec. 1976.

[10] K. Solbach, "The calculation and the measurement of the coupling properties of dielectric image lines of rectangular cross section," *IEEE Trans. Microwave Theory Tech.*, vol. MTT-27, pp. 54–58, Jan. 1979.

[11] T. Trinh and R. Mittra, "Coupling characteristics of planar dielectric waveguides of rectangular cross section," *IEEE Trans. Microwave Theory Tech.*, vol. MTT-29, pp. 875–880, Sept. 1981.

[12] D. Marcuse, "The coupling of degenerate modes in two parallel dielectric waveguides," *Bell Syst. Tech. J.*, vol. 50, pp. 1791–1816, July–Aug. 1971.

[13] T. Trinh and R. Mittra, "Field profile in a single-mode curved dielectric waveguide of rectangular cross section," *IEEE Trans. Microwave Theory Tech.*, vol. MTT-29, pp. 1315–1318, Dec. 1981.

Tsukasa Yoneyama (S'60–M'69) graduated from Tohoku University, Sendai, Japan, in 1959, and received the M.E. and Ph.D. degrees in electrical communication engineering from the same university in 1961 and 1964, respectively.

He is currently an Associate Professor at the Research Institute of Electrical Communication, Tohoku University, where his research interests are concerned with electromagnetic field theory and millimeter-wave integrated circuits.

Dr. Yoneyama is a member of IECE of Japan.

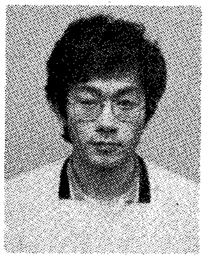

Norio Tozawa graduated from Niigata University, Niigata, Japan, in 1981, and received the M.E. degree in electrical communication engineering from Tohoku University, Sendai, Japan, in 1983. He was mainly concerned with research into millimeter-wave integrated circuits there.

He is presently with Fujitsu Ltd., Kawasaki, Japan.

Shigeo Nishida (SM'59) was born in Nagoya, Japan, on March 7, 1924. He graduated from Tohoku University, Sendai, Japan, in 1949, and received the Ph.D. degree from the same university in 1959.

He was appointed a Research Associate and an Associate Professor at the Research Institute of Electrical Communication, Tohoku University, in 1949 and 1955, respectively. From 1957 to 1959, on leave of absence from Tohoku University, he joined the Microwave Research Institute of the Polytechnic Institute of Brooklyn, Brooklyn, NY, where he was engaged in the research on microwave waveguides and antennas. Since 1964, he has been a Professor at Tohoku University, and his major interests are in microwave and optical-wave transmissions.

A Compact Septum Polarizer

N. CHR. ALBERTSEN AND PER SKOV-MADSEN

***Abstract* — A waveguide polarizer with resonant notches in a septum is investigated. The Wiener-Hopf technique is employed to derive theoretical design data and the results are compared to experiments for a single-notch and a double-notch design. It is concluded that the agreement is good and the design useful for narrowband applications.**

Manuscript received December 29, 1982; revised March 15, 1983. This work was sponsored by the Danish Space Board under Grant 1112-9/81.

N. Chr. Albertsen is with the Laboratory of Applied Mathematical Physics, Technical University of Denmark, Lyngby, Denmark.

P. Skov-Madsen is with the Electromagnetics Institute, Technical University of Denmark, Lyngby, Denmark.

I. Introduction

In antenna systems where circular polarization is required, septum polarizers constitute a simple device for converting linear polarization into circular polarization in the feed waveguide. Examples of broad-band polarizer designs, based mainly on an experimental approach, are found in the literature, e.g., [1] and [2]. In the present paper, a narrow-band polarizer is analyzed analytically, using the Wiener-Hopf technique combined with Galerkin's method, and experimental test results for two specific designs are presented to validate the theoretical analysis.

0018-9480/83/0800-0654$01.00 ©1983 IEEE

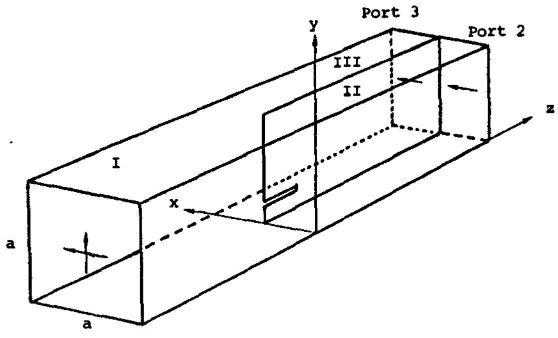

Fig. 1. Geometry of septum polarizer.

The advantage gained is that a more compact design is obtained at the expense of less bandwidth.

II. Formulation of the Problem

The polarizer consists of a rectangular waveguide (inside dimensions $a \times a$) bifurcated by a notched septum, as shown in Fig. 1. The waveguide for $z < 0$ will be denoted Section I, and the two waveguides for $z > 0$ (inside dimensions $a \times (a/2)$) will be denoted Sections II and III. The frequency range is limited by the demand that only the TE_{10} and TE_{01} modes can propagate in Section I. It follows that only a TE_{01} mode can propagate in Sections II and III. For an infinitely thin septum, a TE_{01} mode will propagate unaffected, whereas a TE_{10} mode incident from z negative will be diffracted at $z = 0$. Our purpose is to design the notch such that the TE_{10} mode is totally converted into TE_{01} modes in Sections II and III in phase quadrature with the TE_{01} modes produced by a TE_{01} mode in Section I.

Throughout the analysis it is assumed that the notch is narrow, and therefore only supports an electric field ($\bar{E}_s$) with a y component as illustrated in Fig. 2. It is furthermore assumed, in analogy with the analysis of slot antennas, that $\bar{E}_s$ has a sinusoidal variation in z and standard edge singularities. These properties are summarized in

$$\bar{E}_s = E_0 P(y-d) f_s(z) \hat{y} \tag{1}$$

where E_0 is an arbitrary constant and (see e.g., [3])

$$P(y) = \begin{cases} \dfrac{2b}{\pi\sqrt{b^2 - 4y^2}}, & |y| < \dfrac{1}{2}b \\ 0, & |y| \geq \dfrac{1}{2}b \end{cases} \tag{2}$$

$$f_s(z) = \begin{cases} \sin k(l-z), & 0 \leq z \leq l \\ 0, & z < 0 \text{ and } l \leq z \end{cases} \tag{3}$$

where k is the free-space propagation constant. According to Love's equivalence principle we can replace the notch by a perfect conductor, covered on both sides by a magnetic sheath current. This current will be denoted $E_0\bar{K} = -\hat{n} \times \bar{E}_s$, where $\hat{n}$ is an outward pointing normal vector. We convert $\bar{K}$ into a volume form ($\bar{K}_s$)

$$\bar{K}_s = P(y-d) f_s(z) \left\{ \delta\left(x - \frac{a}{2} -\right) - \delta\left(x - \frac{a}{2} +\right) \right\} \hat{z}. \tag{4}$$

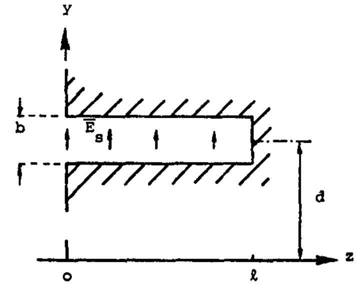

Fig. 2. Geometry of the notch.

The problem can now be summarized as follows. For a given incident TE_{10} mode in Section I we must determine E_0 such that the tangential magnetic field is continuous through the notch, since (4) ensures the continuity of the tangential electric field. When E_0 is found, the scattered field in Sections I, II, and III can be determined.

III. Solution of the Problem

The solution will proceed as follows. We first consider the situation where there is no $\bar{K}_s$, and calculate the field distribution for a TE_{10} mode ($\bar{E}_I^i$) incident on the septum from Section I. The scattered field will consist of TE_{n0} modes only, and we denote the reflected TE_{10} mode $\bar{E}_I^r$ and the z component of the magnetic field on the septum H_s^i. We next consider a situation where (4) is the only source of the fields. We denote the TE_{10} mode excited in Section I $\bar{E}_I^s$, the TE_{01} modes excited in Sections II and III are denoted $\bar{E}_{II}^s$ and $\bar{E}_{III}^s$, and the z component of the magnetic field on the septum (outside the sheath current) H_s^s. Since the structure is symmetric with respect to the plane $x = a/2$ and is being excited by a TE_{10} mode, we can deduce certain symmetries of the total field also. Thus E_y, E_z, and H_x must be symmetrical, E_x, H_y, and H_z antisymmetrical with respect to $x = a/2$. As a consequence, a TE_{01} mode, e.g., will not be excited in Section I. Also due to symmetry, continuity of the magnetic field in the notch is equivalent to the requirement that $H_s^i + E_0 H_s^s$ is zero at the position of the notch. This condition is enforced by taking the moment with the complex conjugate of the expansion function, viz., $P(y-d)f_s^*(z)$, where the conjugation only affects k which is assumed to have a small, negative, imaginary part as customary with the Wiener-Hopf technique [4]. The ensuing equation determines E_0 with which $\bar{E}_I^s$, $\bar{E}_{II}^s$, and $\bar{E}_{III}^s$ must be multiplied to get the scattered modes.

The scattered field produced by an incident TE_{10} mode in Section I has been calculated in [5], and only the result will be quoted here, in a slightly different notation. Let

$$\bar{E}_I^i = \sin\frac{\pi x}{a} e^{-jk_1 z}\hat{y}, \qquad k_1 = \sqrt{k^2 - \left(\frac{\pi}{a}\right)^2} \tag{5}$$

then

$$\bar{E}_I^r = 2\left(\frac{K_0^-(k_1)}{ak_1}\right)^2 \sin\frac{\pi x}{a} e^{jk_1 z}\hat{y}. \tag{6}$$

Here, and everywhere in the following, the time factor $e^{j\omega t}$ is suppressed. The split function $K_0^-(\alpha)$ is the zeroth-order case of the general split function $K_n^-(\alpha)$ discussed in the Appendix. An expression for H_s^i is derived from the scattered E-field, since the incident field does not contribute, and

$$H_s^i = \frac{K_0^-(k_1)}{a\pi\omega\mu}\int_{-\infty}^{\infty}\frac{K_0^-(-\alpha)}{\alpha - k_1}e^{-j\alpha z}\,d\alpha \quad \text{for } x = \frac{a}{2}-. \tag{7}$$

Whenever a field value is evaluated for $x = a/2-$, this is to be interpreted as the limit $x \to (a/2-) - \epsilon$ for $\epsilon \to 0$.

We now turn to the problem of calculating the fields excited by $\bar{K}_s$. In this case, both TE and TM modes of all orders are excited, and it is therefore useful to introduce the electric and magnetic Hertz potentials, $\Pi_E \hat{z}$ and $\Pi_M \hat{z}$, respectively. These potentials must satisfy the equations

$$(\nabla^2 + k^2)\Pi_E = 0 \quad \text{and} \quad (\nabla^2 + k^2)\Pi_M = \frac{j}{\omega\mu}\bar{K}_s \cdot \hat{z}. \tag{8}$$

Furthermore, the Fourier transforms are introduced as

$$\Phi(x, y, \alpha) = \frac{1}{\sqrt{2\pi}}\int_{-\infty}^{\infty}\Pi(x, y, z)e^{j\alpha z}\,dz \tag{9}$$

with suffix E or M as appropriate. Taking the Fourier transforms of (8) results in

$$\left(\frac{\partial^2}{\partial x^2} + \frac{\partial^2}{\partial y^2} + k^2 - \alpha^2\right)\Phi_E = 0 \tag{10}$$

and

$$\left(\frac{\partial^2}{\partial x^2} + \frac{\partial^2}{\partial y^2} + k^2 - \alpha^2\right)\Phi_M = \frac{j}{\omega\mu\sqrt{2\pi}}P(y-d)\left\{\delta\left(x - \frac{a}{2}-\right) - \delta\left(x - \frac{a}{2}+\right)\right\}\tau(\alpha) \tag{11}$$

where

$$\tau(\alpha) = \int_0^l f_s(z)e^{j\alpha z}\,dz = \frac{1}{2}\frac{e^{j\alpha l} - e^{jkl}}{k - \alpha} + \frac{1}{2}\frac{e^{j\alpha l} - e^{-jkl}}{k + \alpha}. \tag{12}$$

The integral transforms are now expanded into Fourier series

$$\Phi_E = \sum_{n=0}^{\infty}\phi_{E,n}(x)\sin\frac{n\pi y}{a}$$
$$\Phi_M = \sum_{n=0}^{\infty}\phi_{M,n}(x)\cos\frac{n\pi y}{a} \tag{13}$$

where the boundary conditions that the tangential electric field must vanish at $y = 0$ and $y = a$ have been used. When (13) is inserted into (10) and (11), these separate into

$$\frac{d^2\phi_{E,n}}{dx^2} + \kappa_n^2\phi_{E,n} = 0$$
$$\frac{d^2\phi_{M,n}}{dx^2} + \kappa_n^2\phi_{M,n} = \tau(\alpha)\rho_n\left\{\delta\left(x - \frac{a}{2}-\right) - \delta\left(x - \frac{a}{2}+\right)\right\} \tag{14}$$

where

$$\kappa_n^2 = k^2 - \left(\frac{n\pi}{a}\right)^2 - \alpha^2 \tag{15}$$

and

$$\rho_n = \frac{j}{\omega\mu\sqrt{2\pi}}\frac{\epsilon_n}{a}\int_0^a \cos\frac{n\pi y}{a}P(y-d)\,dy = \frac{2j}{\omega\mu\sqrt{2\pi}}\epsilon_n\frac{b}{a}\cos\frac{n\pi d}{a}J_0\left(\frac{n\pi b}{2a}\right). \tag{16}$$

Here ϵ_n is Neumann's symbol and J_0 is the Bessel function of order zero. The complete solution to (14), taking into account symmetry, is

$$\phi_{E,n} = \begin{cases} B\sin\kappa_n x \\ B\sin\kappa_n(a-x) \end{cases}$$
$$\phi_{M,n} = \begin{cases} A\cos\kappa_n x, & x < \frac{a}{2} \\ -A\cos\kappa_n(a-x), & \frac{a}{2} < x. \end{cases} \tag{17}$$

Integration of the inhomogeneous term in (14) yields

$$\phi'_{M,n}\left(\frac{a}{2}\right) + A\kappa_n\sin\frac{\kappa_n a}{2} = \rho_n\tau(\alpha). \tag{18}$$

A prime denotes here, and in the following, differentiation with respect to x. From (13) we find that the Fourier transforms of the field components E_z and H_y can be expanded into odd Fourier series, whereas E_y and $\partial E_y/\partial x$ have even Fourier series. Using the small letters $e_{z,n}$, $h_{y,n}$, $e_{y,n}$, and $e'_{y,n}$ to denote the coefficients, we obtain, inserting (17)

$$e_{z,n}\left(\frac{a}{2}\right) = (k^2 - \alpha^2)B\sin\frac{\kappa_n a}{2} \tag{19}$$

$$h_{y,n}\left(\frac{a}{2}-\right) = j\left(-\omega\epsilon B\kappa_n + \alpha\frac{n\pi}{a}A\right)\cos\frac{\kappa_n a}{2} \tag{20}$$

$$e_{y,n}\left(\frac{a}{2}\right) = -j\alpha\frac{n\pi}{a}B\sin\frac{\kappa_n a}{2} + j\omega\mu\phi'_{M,n}\left(\frac{a}{2}\right) \tag{21}$$

$$e'_{y,n}\left(\frac{a}{2}-\right) = -j\kappa_n\left(\alpha\frac{n\pi}{a}B + \omega\mu A\kappa_n\right)\cos\frac{\kappa_n a}{2}. \tag{22}$$

We insert (18) into (21) and combine (21) and (22) into

$$e'_{y,n}\left(\frac{a}{2}-\right) = \frac{2}{a}K_n(\alpha)\left(-j\omega\mu\rho_n\tau(\alpha) + e_{y,n}\left(\frac{a}{2}\right)\right) \tag{23}$$

and (19), (20), and (21) into

$$h_{y,n}\left(\frac{a}{2}-\right) = \frac{2}{a}K_n(\alpha)\frac{1}{\kappa_n^2}\left(j\alpha\frac{n\pi}{a}\rho_n\tau(\alpha) - \frac{\alpha}{\omega\mu}\frac{n\pi}{a}e_{y,n}\left(\frac{a}{2}\right) - j\omega\epsilon\frac{k_n^2}{k^2}e_{z,n}\left(\frac{a}{2}\right)\right) \tag{24}$$

where

$$K_n(\alpha) = \frac{\frac{1}{2}\kappa_n a\cos\left(\frac{1}{2}\kappa_n a\right)}{\sin\left(\frac{1}{2}\kappa_n a\right)} \tag{25}$$

and

$$k_n^2 = k^2 - \left(\frac{n\pi}{a}\right)^2. \tag{26}$$

In order to convert (23) and (24) into equations of Wiener-Hopf type we split each transform into two functions, e.g., $e_{z,n} = e_{z,n}^- + e_{z,n}^+$, where the superscript $-$ indicates that the transformation integral is over the range $-\infty < z < 0$, whereas $+$ indicates the range $0 < z < \infty$. At $x = a/2$ the tangential electric field must be zero for $z > 0$ and all field components and their derivatives must be continuous for $z < 0$. From the symmetry we deduce that H_y and $\partial E_y/\partial x$ are zero for $z < 0$ and $x = a/2$. Consequently a superscript $+$ can be added to $e'_{y,n}(a/2-)$ and $h_{y,n}(a/2-)$ in (23) and (24), and a superscript $-$ to $e_{y,n}(a/2)$ and $e_{z,n}(a/2)$. The edge conditions at $z = 0$ ensure that the functions in (23) have the proper behavior for $\alpha \to \infty$, and the equation can be solved by standard Wiener-Hopf technique [4]

$$e_{y,n}^-\left(\frac{a}{2}\right) = j\omega\mu\rho_n\frac{T_n^-(\alpha)}{K_n^-(\alpha)}. \tag{27}$$

The factorization of $K_n(\alpha)$ is considered in the Appendix, where also an expression for $T_n^-(\alpha)$ is given, derived from the separation of $T_n(\alpha) = T_n^-(\alpha) + T_n^+(\alpha) = K_n^-(\alpha)\tau(\alpha)$. Inserting (27) into (24) we obtain, after rearranging

$$h_{y,n}^+\left(\frac{a}{2}-\right)\frac{k_n-\alpha}{K_n^+(\alpha)} = \frac{2}{a}\frac{K_n^-(\alpha)}{k_n+\alpha}\left\{j\alpha\frac{n\pi}{a}\rho_n\frac{T_n^+(\alpha)}{K_n^-(\alpha)} - j\omega\epsilon\frac{k_n^2}{k^2}e_{z,n}^-\left(\frac{a}{2}\right)\right\}. \tag{28}$$

This equation is also of Wiener-Hopf type and we find

$$e_{z,n}^-\left(\frac{a}{2}\right) = \frac{a}{2j\omega\epsilon}\frac{k^2}{k_n^2}\frac{k_n+\alpha}{K_n^-(\alpha)}U_n^-(\alpha) \tag{29}$$

where $U_n^-(\alpha)$ is derived from the separation

$$U_n(\alpha) = U_n^-(\alpha) + U_n^+(\alpha) = j\alpha\rho_n\frac{2n\pi}{a^2}\frac{T_n^+(\alpha)}{k_n+\alpha}. \tag{30}$$

This can be carried out by inspection, and

$$U_n^-(\alpha) = -j\rho_n\frac{2n\pi}{a^2}\frac{k_nT_n^+(-k_n)}{\alpha+k_n}. \tag{31}$$

Having found $e_{z,n}(a/2)$ and $e_{y,n}(a/2)$, we can determine A and B from (19) and (21) and, via (17) and (13), we finally obtain the potentials Π_E and Π_M from the inverse Fourier transforms as

$$\Pi_E = -\frac{\omega\mu}{\sqrt{2\pi}}\int_{-\infty}^{\infty}\sum_{n=0}^{\infty}\rho_n\frac{n\pi}{a} \cdot\frac{T_n^+(-k_n)\sin\kappa_n x\sin\frac{n\pi y}{a}}{k_n(k^2-\alpha^2)K_n^-(\alpha)\sin\left(\frac{1}{2}\kappa_n a\right)}e^{-j\alpha z}d\alpha, \qquad x < \frac{a}{2} \tag{32}$$

$$\Pi_M = \frac{1}{\sqrt{2\pi}}\int_{-\infty}^{\infty}\sum_{n=0}^{\infty}\rho_n\left(T_n^+(\alpha)+\left(\frac{n\pi}{a}\right)^2\frac{\alpha T_n^+(-k_n)}{k_n(k^2-\alpha^2)}\right) \cdot\frac{\cos\kappa_n x\cos\frac{n\pi y}{a}}{\kappa_nK_n^-(\alpha)\sin\left(\frac{1}{2}\kappa_n a\right)}e^{-j\alpha z}d\alpha, \qquad x < \frac{a}{2}. \tag{33}$$

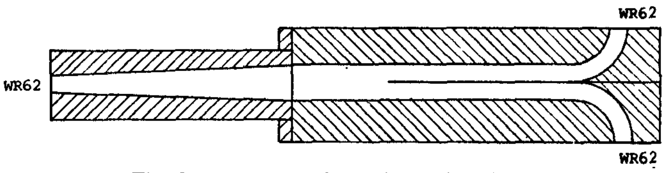

Fig. 3. Geometry of experimental model.

From (32) and (33) we can find $\bar{E}_{\mathrm{I}}^s$, $\bar{E}_{\mathrm{II}}^s$, and $\bar{E}_{\mathrm{III}}^s$. Evaluating the integrals by residue calculus we find

$$\bar{E}_{\mathrm{I}}^s = \omega\mu\sqrt{2\pi}\,\rho_0\frac{4K_0^-(k_1)T_0^-(-k_1)}{a^2k_1}\sin\frac{\pi x}{a}e^{jk_1z}\hat{y} \tag{34}$$

$$\bar{E}_{\mathrm{II}}^s = -\bar{E}_{\mathrm{III}}^s = -\omega\mu\sqrt{2\pi}\,\rho_1\frac{\pi}{a^2k_1} \cdot\left\{\tau(k_1)+\frac{\tau(-k_1)}{(K_1^-(k_1))^2}-\frac{T_1^-(k_1)+T_1^-(-k_1)}{K_1^-(k_1)}\right\} \cdot\sin\frac{\pi y}{a}e^{-jk_1z}\hat{x}. \tag{35}$$

The z component of the magnetic field at $x = a/2-$ is found from (33) as

$$H_s^s = \frac{1}{\sqrt{2\pi}}\sum_{n=0}^{\infty}\frac{2\rho_n}{a}\cos\frac{n\pi y}{a} \cdot\int_{-\infty}^{\infty}\left\{(k^2-\alpha^2)T_n^+(\alpha)+\left(\frac{n\pi}{a}\right)^2\frac{\alpha}{k_n}T_n^+(-k_n)\right\} \cdot K_n^+(\alpha)\frac{e^{-j\alpha z}}{\kappa_n^2}d\alpha. \tag{36}$$

Finally E_0 is found as

$$E_0 = -\frac{b(f_s, H_s^i)}{(P(y-d)f_s, H_s^s)} \tag{37}$$

where (,) is an inner product. Expressions for the nominator and denominator may be found in the Appendix.

IV. Results

The scattered modes were calculated for a large number of parameter values, using the theory developed in the preceding section. As a check on the accuracy, the total output power was compared to the input power, and the discrepancy was in all cases less than 0.01 dB. For a number of notch lengths, contour plots for the reflection coefficient were calculated as function of width and displacement of the notch. It was found that with lengths in the range $l/a = 0.4$ to $l/a = 0.7$, where the values have been normalized with respect to the waveguide height (a), a combination of b and d existed, for which the polarizer was matched, but the phase of the transmitted modes was in all cases close to $-140°$ in Section II. The largest bandwidth was obtained for small values of l and consequently the following combination was selected for further analysis: $l/a = 0.421$, $d/a = 0.347$, and $b/a = 0.042$.

To verify the calculations a septum polarizer was manufactured in P-band with $a = 15.8$ mm. The two waveguide Sections II and III were continued into E-plane bends with flanges in standard P-band waveguide (WR62) (see Fig. 3),

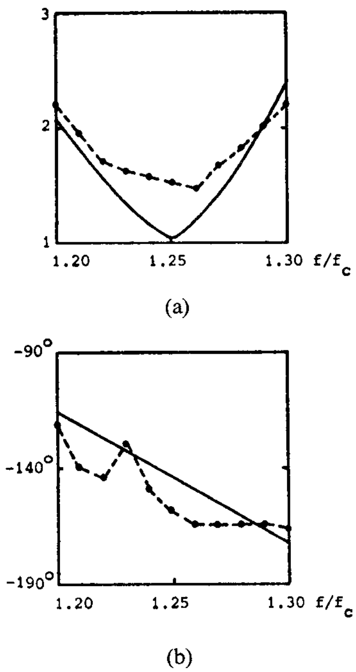

Fig. 4. (a) VSWR for Port 1 and (b) phase of S_{12} for septum polarizer with one notch. —— theory, ----- experiment.

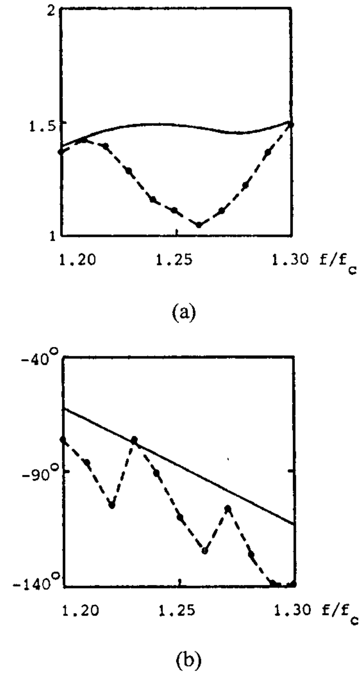

Fig. 5. (a) VSWR for Port 1 and (b) phase of S_{12} for septum polarizer with two notches. —— theory, ----- experiment.

which also shows the transition used between WR62 and the square waveguide as a 3λ long, tapered section. During the measurements the transition could be mounted in orthogonal positions to switch between Ports 1 and 4 (see Fig. 1). First two matched loads were placed at Ports 2 and 3, and $|S_{11}|$ and $|S_{44}|$ measured with a slotted line. The value of $|S_{44}|$ (~ -30 dB) confirmed that the transition was good and that the interaction between an incident TE_{01} mode and the septum is negligible. The value of the VSWR was calculated from $|S_{11}|$ and is compared to the theoretical value in Fig. 4(a) as a function of the frequency, normalized with respect to the cutoff frequency (f_c) for the TE_{10} mode, and good agreement is found, except at the minimum of the VSWR curve. The discrepancy here is believed to be caused by the finite thickness of the septum. The absolute phases of S_{12} and S_{13} could not be measured directly with the experimental setup used, since the lengths of the phase paths in the transition at Port 1 and the E-plane bends at Ports 2 and 3 were unknown. Use was made of the fact, however, that these would affect the phases of S_{12} and S_{42} similarly. Therefore, the phase difference between the signal transmitted from Port 1 to Port 2 and that from Port 4 to Port 2 must equal the phase difference between S_{12} and S_{42}. The phases were measured with a HP8410 Network Analyzer, and the result is compared to the theoretical result in Fig. 4(b), where it has been assumed that the phase of S_{42} is zero. The agreement is reasonably good, considering that the latter assumption is only approximate due to the finite thickness of the septum and that the measuring accuracy is estimated to be $\pm 10°$.

As mentioned above the phase of the transmitted mode is far from the required $\pm 90°$. To correct the phase, either a dielectric membrane may be used as in [2], or more degrees of freedom must be introduced into the design. The theory in the preceding section is easily extended to an arbitrary number of notches, although the amount of computation involved increases rapidly, since also mutual coupling between the notches must be included. The latter approach was considered the more interesting, and a septum with two notches was designed. In this case the number of parameters is so large that a systematic survey of the polarizer characteristics cannot be made. A large number of contour plots for the reflection coefficient and the phase of the transmitted modes were made as a function of the width (b_1) and the displacement (d_1) for notch No. 1 for various combinations of the remaining parameters, and the optimum combination found was chosen. The particular design investigated has the following data: $l_1/a = 0.484$, $d_1/a = 0.017$, $b_1/a = 0.021$, $l_2/a = 0.379$, $d_2/a = 0.500$, and $b_2/a = 0.084$, where the suffix refers to the notch number. The theoretical and experimental results for this design are compared in Fig. 5. The VSWR is here acceptable over a broad band, and the useful bandwidth is therefore limited by the phase slope only. With a circularly polarized mode incident from Section I, a 20-dB separation between Ports 2 and 3 can be achieved over a 3.7-percent bandwidth, e.g., whereas a 26 dB separation is obtained over 1.8-percent bandwidth only. Also here, a discrepancy is found between theory and experiment for small VSWR values, but this time in favor of the experiment. Again we attribute the differences to the finite thickness of the septum (0.3 mm), which is even more important in this case where b_1 is comparable to the thickness. The results show that it is possible to obtain an isolation between Ports 2 and 3 that is better than the theoretically found 20 dB.

V. Conclusion

The theory for a notched septum waveguide polarizer has been developed, and theoretical results have been compared to experimental results for two designs. It has been shown that with one notch, good isolation (~ 20 dB) can be obtained over a 3.2-percent bandwidth, but no control of the phase is possible and the design is not useful for circular polarization. With a two-notch design, good isolation can be obtained over a wider band, and the phase can be controlled such that a 20-dB separation of circular polarization can be obtained over a 3.7-percent bandwidth.

Appendix

An important step in the solution of the Wiener-Hopf problem discussed, is the factorization of the complex function $K_n(\alpha)$ into a product $K_n^+(\alpha)K_n^-(\alpha)$, where

$$K_n(\alpha)=\frac{\frac{1}{2}\kappa_n a\cos\left(\frac{1}{2}\kappa_n a\right)}{\sin\left(\frac{1}{2}\kappa_n a\right)},\qquad \kappa_n=\sqrt{k_n^2-\alpha^2} \quad \text{(A1)}$$

and

$$k_n=\begin{cases}\sqrt{k^2-\left(\frac{n\pi}{a}\right)^2}, & k\geqslant\frac{n\pi}{a}\\ -j\sqrt{\left(\frac{n\pi}{a}\right)^2-k^2}, & k<\frac{n\pi}{a}.\end{cases} \quad \text{(A2)}$$

The branch cuts for κ_n are from k_n to infinity in the upper halfplane and from $-k_n$ to infinity in the lower halfplane, and $\kappa_n=k_n$ for $\alpha=0$. Following standard procedure [4] we demand that $K_n^+(\alpha)$ is analytic without zeroes in the upper halfplane and has algebraic behavior for $\alpha\to\infty$ here, with similar demands on $K_n^-(\alpha)$ in the lower halfplane. The result is (cf. [4, p. 123])

$$K_n^-(\alpha)=K_n^+(-\alpha)=\prod_{p=1}^{\infty}\frac{p\left(\alpha+\alpha_{n,p-1/2}\right)}{\left(p-\frac{1}{2}\right)\left(\alpha+\alpha_{n,p}\right)} \quad \text{(A3)}$$

where

$$\alpha_{n,p}=\begin{cases}\sqrt{k_n^2-\left(\frac{2p\pi}{a}\right)^2}, & k_n^2\geqslant\left(\frac{2p\pi}{a}\right)^2\\ -j\sqrt{\left(\frac{2p\pi}{a}\right)^2-k_n^2}, & k_n^2<\left(\frac{2p\pi}{a}\right)^2.\end{cases} \quad \text{(A4)}$$

In (27), the function $T_n^-(\alpha)$ is required. It is derived by separation of

$$T_n(\alpha)=\tfrac{1}{2}K_n^-(\alpha)\left(\frac{e^{j\alpha l}-e^{jkl}}{k-\alpha}+\frac{e^{j\alpha l}-e^{-jkl}}{k+\alpha}\right). \quad \text{(A5)}$$

The separation is made with Cauchy's theorem [4], and closing the integral in the upper halfplane we obtain

$$\begin{aligned}T_n^-(\alpha)=&-\frac{1}{2}e^{jkl}\frac{K_n^-(\alpha)-K_n^-(k)}{k-\alpha}\\ &-\frac{1}{2}e^{-jkl}\frac{K_n^-(\alpha)-K_n^-(-k)}{k+\alpha}\\ &+k\sum_{p=1}^{\infty}\frac{e^{-j\alpha_{n,p}l}\left(k_n^2-\alpha_{n,p}^2\right)}{\left(\alpha+\alpha_{n,p}\right)\left(k^2-\alpha_{n,p}^2\right)\alpha_{n,p}K_n^-\left(\alpha_{n,p}\right)}.\end{aligned} \quad \text{(A6)}$$

The inner products in (37) are evaluated as follows:

$$\begin{aligned}\left(f_s,H_s^i\right)&=\int_0^l\sin k^*(l-z)H_s^i(z)\,dz\\ &=K_0^-(k_1)\frac{j}{\omega\mu a}\left\{F\left(K_0^-(k);-k_1\right)+2k\sum_{p=1}^{\infty}\frac{P_{0,p}}{\left(\alpha_{0,p}-k_1\right)}\right\}\end{aligned} \quad \text{(A7)}$$

$$\begin{aligned}\frac{1}{b}\left(P(y-d)f_s,H_s^s\right)&=\frac{1}{b}\int_0^l\int_0^a P(y-d)\cdot\sin k^*(l-z)H_s^s(y,z)\,dy\,dz\\ &=\frac{1}{\sqrt{2\pi}}\sum_{n=0}^{\infty}\frac{2\rho_n}{a}\cdot\cos\frac{n\pi d}{a}J_0\left(\frac{n\pi b}{2a}\right)I_n\end{aligned} \quad \text{(A8)}$$

where

$$\begin{aligned}\mathrm{I}_0=2\pi j\Bigg\{&\frac{1}{8k}\left(\left(K_0^-(k)e^{jkl}\right)^2-\left(K_0^-(-k)e^{-jkl}\right)^2\right)\\ &-\frac{1}{4}\left(2jl+K_0^-(k)\left.\frac{dK_0^-(\alpha)}{d\alpha}\right|_{\alpha=-k}+K_0^-(-k)\left.\frac{dK_0^-(\alpha)}{d\alpha}\right|_{\alpha=k}\right)\\ &+\sum_{p=1}^{\infty}\frac{k}{\alpha_{0,p}}\frac{k}{k^2-\alpha_{0,p}^2}\\ &-\sum_{p=1}^{\infty}kP_{0,p}F\left(K_0^-(k);\alpha_{0,p}\right)\\ &-k^2\sum_{x=1}^{\infty}\sum_{x=1}^{\infty}\frac{P_{0,p}P_{0,q}}{\alpha_{0,p}+\alpha_{0,q}}\Bigg\}\end{aligned} \quad \text{(A9)}$$

and

$$
\begin{aligned}
\mathrm{I}_n = \frac{2\pi j}{k_n}\Bigg\{ & \frac{1}{2}\frac{k^2}{k^2-k_n^2} + \frac{1}{8}K_n^-(k_n)\big((k+k_n)e^{jkl} \\
& + (k-k_n)e^{-jkl}\big)F(K_n^-(k); -k_n) - \frac{1}{4}ke^{-jk_nl} \\
& \cdot \big(F(1;k_n) + K_n^-(-k_n)F(K_n^-(k);k_n)\big) \\
& + \sum_{p=1}^{\infty}\frac{k_nk^2}{\alpha_{n,p}\left(k^2-\alpha_{n,p}^2\right)} - \frac{1}{2}k_nk\sum_{p=1}^{\infty}\frac{e^{-j\alpha_{n,p}l}}{\alpha_{n,p}K_n^-(\alpha_{n,p})} \\
& \cdot F\big(K_n^-(k)+K_n^-(\alpha_{n,p}); \alpha_{n,p}\big) \\
& - \frac{1}{2}K_n^-(-k_n)e^{-jk_nl}\sum_{p=1}^{\infty}\frac{k^2P_{n,p}}{\alpha_{n,p}+k_n} \\
& - \sum_{p=1}^{\infty}\sum_{q=1}^{\infty}\frac{k_nk^2P_{n,q}e^{-j\alpha_{n,p}l}}{(\alpha_{n,p}+\alpha_{n,q})\alpha_{n,p}K_n^-(\alpha_{n,p})} \\
& + \frac{1}{4}K_n^-(k_n)k\left(k^2-k_n^2\right)F(1;k_n)\sum_{p=1}^{\infty}\frac{P_{n,p}}{\alpha_{n,p}-k_n} \\
& + \frac{1}{2}kk_n\sum_{p=1}^{\infty}\frac{e^{-j\alpha_{n,p}l}}{\alpha_{n,p}}F(1;\alpha_{n,p}) \\
& + \left(k^2-k_n^2\right)T_n^+(-k_n)\Bigg(\frac{1}{2}K_n^-(-k_n)\frac{ke^{-jk_nl}}{k^2-k_n^2} \\
& + k\sum_{p=1}^{\infty}\frac{\alpha_{n,p}}{k_n^2-\alpha_{n,p}^2}P_{n,p} - \frac{1}{2}\frac{k^2}{k^2-k_n^2}F(K_n^-(k);0) \\
& + \frac{1}{4}K_n^-(k_n)F(1;k_n)\Bigg)\Bigg\}, \qquad n>0.
\end{aligned} \tag{A10}
$$

For convenience the following abbreviations are used:

$$F(f(k);\alpha) = \frac{f(k)e^{jkl}}{k-\alpha} + \frac{f(-k)e^{-jkl}}{k+\alpha} \tag{A11}$$

$$P_{n,p} = \frac{e^{-j\alpha_{n,p}l}}{\alpha_{n,p}K_n^-(\alpha_{n,p})}\frac{k_n^2-\alpha_{n,p}^2}{k^2-\alpha_{n,p}^2}. \tag{A12}$$

References

[1] E. C. Nygren, "Shaped-beam, frequency-reuse feed arrays for offset-fed reflectors," presented at the AIAA 8th Communications Satellite Systems Conf., Apr. 20–24, Orlando, FL, 1980.

[2] M. H. Chen and G. N. Tsandoulas, "A wide-band square-waveguide array polarizer," *IEEE Trans. Antennas Propagat.*, vol. AP-21, pp. 389–391, May 1973.

[3] P. K. Park and S. W. Lee, "Characterization of slots in rectangular waveguide by method of moments with proper edge condition," in *APS Symp. Dig.* (Albuquerque, NM), 1982, pp. 572–574.

[4] B. Noble, *Methods Based on Wiener-Hopf Technique.* New York: Pergamon Press, 1958.

[5] D. S. Jones, *The Theory of Electromagnetism.* Oxford: Pergamon Press, 1964.

N. Chr. Albertsen was born in Frederiksberg, Denmark, in 1946. He received the M.Sc.E.E. and Ph.D. degrees from the Technical University of Denmark, Lyngby, in 1970 and 1975, respectively.

From 1970 to 1975 he was associated with the Electromagnetics Institute, Technical University of Denmark. Since 1975 he has been with the Laboratory of Applied Mathematical Physics, Technical University of Denmark as Associate Professor. He has been a member of the board of directors of TICRA A/S since the company was formed in 1971.

Per Skov-Madsen was born April 18, 1956. He received the M.S. in electrical engineering from the Technical University of Denmark in 1981.

Since 1981 he has been employed at the Electromagnetics Institute at the Technical University of Denmark.